

## Getting the MAX out of Computational Models: The Prediction of Unbound-Brain and Unbound-Plasma Maximum Concentrations

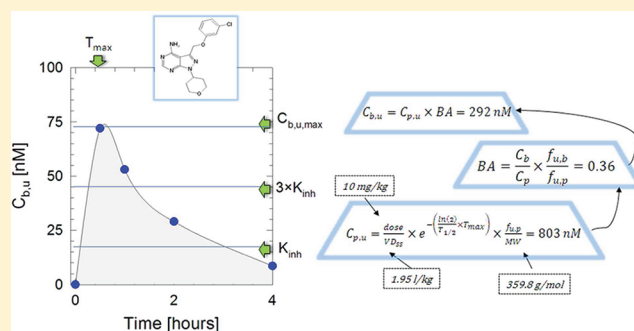
Scot Mente,\* Angela Doran, and Travis T. Wager

Groton Laboratories, Pfizer Worldwide Research and Development, 1 Eastern Point Road, Groton, Connecticut 06340, United States

## Supporting Information

**ABSTRACT:** The objective of this work was to establish that unbound maximum concentrations may be reasonably predicted from a combination of computed molecular properties assuming subcutaneous (SQ) dosing. Additionally, we show that the maximum unbound plasma and brain concentrations may be projected from a mixture of in vitro absorption, distribution, metabolism, excretion experimental parameters in combination with computed properties (volume of distribution, fraction unbound in microsomes). Finally, we demonstrate the utility of the underlying equations by showing that the maximum total plasma concentrations can be projected from the experimental parameters for a set of compounds with data collected from clinical research.

**KEYWORDS:** ADME, blood–brain barrier, brain availability,  $C_{max}$ , fraction unbound, volume of distribution



The desire to guide medicinal chemistry design and synthesis toward favorable chemical space has led to a variety of computational approaches. These include the seminal work of Lipinski<sup>1</sup> as well as others<sup>2,3</sup> who have attempted to define criteria as to which compounds are favorable with respect to drug-likeness. These criteria are often based upon calculatable physical–chemical properties and allow for the straightforward application of such criteria to the evaluation of virtual compounds. Other methods have been developed in an attempt to directly model ADME (absorption, distribution, metabolism, and excretion) parameters from a molecular structure and have included the prediction of clearance,<sup>4</sup> bioavailability,<sup>5</sup> and central nervous system (CNS) penetration.<sup>6,7</sup>

Blood–brain barrier modeling has proven particularly challenging. Previous computational models have been developed to predict CNS penetration via estimation of the total brain-to-plasma concentration ratio  $C_b:C_p$ .<sup>6–10</sup> However, a compound's affinity for plasma proteins and brain tissue may also greatly affect its target exposure in both the brain and the plasma, rendering  $C_b:C_p$  values insufficient as a stand-alone parameter. Whereas previous studies have focused on the concentration ratios, it is the concept of the maximum free concentration ( $C_{max,u}$ ) of a drug that is of interest in the present work.

Here, we explore the value of using multiple combined computational models as they pertain to a common preclinical CNS experiment: single dose SC injections to determine both neuroexposure and concomitant peripheral exposure. The maximum free concentration of a drug following single subcutaneous (SC) dosing may be expressed as a function of

compound dose (mg/kg) and steady-state volume of distribution ( $VD_{ss}$ ). If one can calculate  $VD_{ss}$  and the fraction of compound unbound in plasma ( $f_{u,p}$ ) from the molecular structure, then an estimate of the maximum free plasma concentration ( $C_{max,p,u}$ ) should be viable. For a peripherally acting drug, this method may be used to estimate the ratio of free drug exposure (maximum unbound plasma compound concentration,  $C_{max,p,u}$ ) to binding/functional activity at the intended biological target. Projected  $C_{max,p,u}$  values may also be used to calculate the therapeutic index for an off-target pharmacology and also help select proper doses for in vivo studies. Furthermore, if the brain availability (BA) can be calculated, then an estimate of the drug's free brain concentration (maximum unbound brain compound concentration,  $C_{max,b,u}$ ) should also be possible. Computational models for both  $VD_{ss}$ <sup>11</sup> and total B/P<sup>6–10</sup> have been the subject of previous computational studies and provide the foundation for this work.

The " $C_{max,u}$  equation" can be formulated as:

$$C_{max,p,u} = \frac{\text{dose}}{cVD_{ss}} \times e^{-\left[\frac{\ln(2)}{T_{1/2}} \times T_{max}\right]} \times \frac{f_{u,p}}{MW} \quad (1)$$

Here, we make the key assumption that the concentration from any dosing study may be normalized to a fixed dose (10 mg/kg); hence, PK is linear across doses. For example, if a drug was dosed at 50 mg/kg resulting in a  $C_{max,p}$  of 100 nM,

Received: February 3, 2012

Accepted: May 16, 2012

Published: May 16, 2012

normalization to a 10 mg/kg would yield a normalized exposure of 20 nM. This enables a straightforward comparison of  $C_{\max,p}$  across published or internal data sets, where dosing regimens may vary. Additionally, we use a model for the calculated volume of distribution,  $cVD_{ss}$ , based on the previously published models.<sup>11</sup>  $T_{1/2}$  is the half-life of compound, and  $T_{\max}$  is the time of maximum drug concentration as illustrated in Figure 1. These parameters are

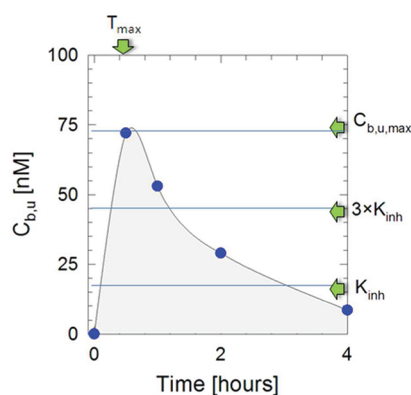


**Figure 1.** Schematic area under the compound concentration–time curve (AUC).

calculated from blood clearance, which is, in turn, calculated using a model for microsomal clearance. Further details of this computation are provided in the Supporting Information. MW is the molecular weight of the compound.

Calculated  $f_{u,p}$  and fraction unbound in brain ( $f_{u,b}$ ) values were determined via correlation between measured  $f_{u,p}$  and  $f_{u,b}$  values with calculated lipophilicity. Correlations between  $f_{u,p}$  and  $f_{u,b}$  with a variety of physicochemical properties revealed a relationship between these values and lipophilicity, as illustrated by the correlation with the computed  $\text{ElogD}$ <sup>12</sup> ( $c\text{ElogD}$ ) in Figure 2. For the set of compounds in Table 1, the  $\log(f_{p,u})$

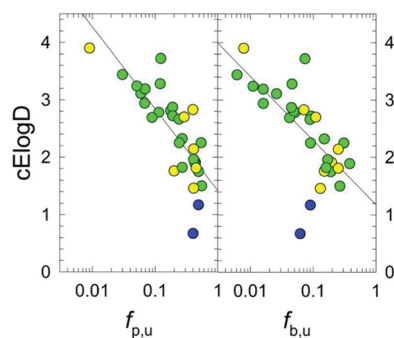


**Figure 2.** Correlation between fraction unbound plasma ( $f_{u,p}$ ) and fraction unbound brain ( $f_{u,b}$ ) with the calculated  $\text{ElogD}$  ( $c\text{ElogD}$ ). Symbol coloring corresponds to the predicted ionization of the compound at pH 7.4; green symbols represent neutral compounds, yellow symbols represent weakly basic compounds, and blue symbols represent strongly basic ( $\text{p}K_a \geq 8$ ).

values are well correlated ( $R^2 = 0.63$ ;  $\text{MSE} = 0.07$ ) with the  $c\text{ElogD}$  parameter and other measures of lipophilicity such as  $\text{ClogP}$  ( $R^2 = 0.48$ ;  $\text{MSE} = 0.10$ ). Other physical properties such as MW, TPSA, and hydrogen bond donor/acceptor counts did not have statistically significant correlations. Although a similar relationship exists for  $f_{u,b}$  and  $c\text{ElogD}$  ( $R^2 = 0.48$ ;  $\text{MSE} = 0.12$ ),

the correlation does not hold for strongly basic compounds (represented as blue symbols) with  $c\text{ElogD}$  values less than 1.5. This likely reflects the positive correlation between the degree of ionization of a compound and that compound's corresponding affinity for brain tissue/phospholipid binding, an effect previously pointed out by Laneskij and co-workers.<sup>13</sup> Removal of those two compounds from the correlation yields better regression results ( $R^2 = 0.67$ ;  $\text{MSE} = 0.08$ ) for the remaining set of compounds, which are either weakly basic or neutral.

For this work, we used the following relationships to predict fraction unbound values based upon the calculated  $\text{ElogD}$ :

$$\log(cf_{u,p}) = 0.34 - 0.44 \times c\text{ElogD} \quad (2)$$

$$\log(cf_{u,b}) = -0.32 - 0.35 \times c\text{ElogD} \quad (3)$$

These correlations have been used to predict fraction unbound values for compounds with  $c\text{ElogD}$  values greater than 1.0. Below this value, a compound is represented by a fixed value and set at 1 (since compounds cannot be over 100% free).

On average, an overestimation of  $C_{\max,p,u}$  is observed for the training set (Table 1); thus, an additional empirical correction factor was applied to normalize the data (eq 4).

$$\log(cC_{\max,p,u}) = -0.59 + 1.06 \times \log(cC_{\max,p,u}) \quad (4)$$

For CNS targeting molecules, it is the free brain concentration ( $C_{\max,b,u}$ ) that is of consequence<sup>14,15</sup> and is what we wish to estimate. Again, we make a similar assumption that  $C_{\max,b,u}$  from single oral dosing studies may be normalized to a fixed dose of 10 mg/kg (linear neuropharmacokinetics across doses).

$$C_{\max,b,u} = C_{\max,p,u} \times \text{cBA} \quad (5)$$

where calculated BA is the ratio  $C_{b,u} : C_{p,u}$  as defined<sup>16</sup>

$$\text{cBA} = \frac{\text{AUC}_b}{\text{AUC}_p} \times \frac{f_{u,b}}{f_{u,p}} = \frac{C_{b,u}}{C_{p,u}} \quad (6)$$

Here, the  $C_b : C_p$  is the total brain/plasma concentration ratio that has typically been used to model brain penetration. The inclusion of  $f_{u,p}$  and  $f_{u,b}$  terms in formulating the “BA” represents an important distinction compared to B/P values and underlies a shift in past modeling efforts.<sup>6</sup> Furthermore, this view of optimizing drugs using the parameters defined in eqs 1–6 is now different than typical CNS models<sup>6–10</sup> and requires an assessment of four parameters:  $\text{VD}_{ss}$ ,  $f_{u,p}$ ,  $f_{u,b}$ , and  $C_b : C_p$ . No published data set exists with all of those parameters experimentally determined, along with reported free brain drug concentrations. For this reason, we demonstrate feasibility of predicting  $C_{\max,p,u}$  and  $C_{\max,b,u}$  for a set of proprietary compounds from the CK1 $\delta/\epsilon$  project for which values for  $C_{\max,p,u}$ ,  $C_{\max,b,u}$ ,  $f_{u,p}$ , and  $f_{u,b}$  have been collected. These data are summarized in Table 1.

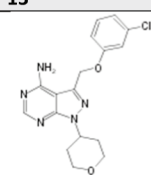
An example workflow for how the  $cC_{\max,p,u}$  and  $cC_{\max,b,u}$  values are derived is provided in Table 2 for compound 13. An Excel spreadsheet containing the calculations for all compounds in Table 1 is provided in the Supporting Information along with a more detailed explanation of the workflow. The correlation between the observed concentration values for the free plasma and free brain is shown in Figure 3. Here, the  $x$ -axis is the observed in vivo concentrations ( $C_{\max,p,u}$  Figure 3a; and  $C_{\max,b,u}$  Figure 3b) plotted versus the corresponding predicted  $cC_{\max,p,u}$

Table 1. Casein Kinase Compound Properties and Exposure Data

CMPD	MW	$C_{\max,p,u}$ (nM)	$C_{\max,b,u}$ (nM)	$C_b:C_p$	predicted values					
					cVDss (l/kg)	$cC_b:C_p$	cElogD	$cC_{\max,p,u}^a$ (nM)	$cC_{\max,b,u}^a$ (nM)	
training set										
1	338	1521	12	0.05	2.82	0.13	0.67	3352	273	
2	443	2816	27	0.02	1.48	0.04	1.50	2323	62	
3	337	271	72	0.9	1.70	0.29	3.28	249	77	
4	419	1646	117	0.13	2.69	0.10	1.91	907	69	
5	239	1448	1606	1.8	1.62	1.08	2.78	1149	1106	
6	279	543	383	1.6	1.51	0.54	3.11	642	340	
7	271	1087	400	0.8	1.35	1.41	2.69	1168	1441	
8	309	359	140	1.4	2.00	1.8	2.81	461	784	
9	323	332	137	1.7	2.19	0.98	2.87	396	374	
10	281	200	66	1.7	1.62	3.06	2.94	459	1359	
11	309	1525	784	0.9	2.04	1.30	2.25	777	831	
12	297	562	193	0.7	1.51	1.02	2.72	476	450	
13	360	180	88	2.1	1.95	0.91	3.19	309	292	
14	416	251	85	1.9	4.71	0.65	2.83	165	107	
15	300	275	66	2.7	1.78	2.33	3.24	347	843	
16 <sup>b</sup>	513	80	784	0.04	2.09	0.06	3.90	111	8	
17	269	2630	193	0.79	1.20	0.44	2.66	1304	496	
18 <sup>b</sup>	491	517	88	0.04	0.78	0.12	3.72	243	34	
19 <sup>c</sup>	256	10364	5385	1.3	1.51	0.29	1.75	1830	378	
test set										
20	433	673	69	0.3	2.40	0.15	2.7	320	45	
21	404	1066	825	1.1	2.19	0.33	2.14	594	160	
22	282	117	24	1.2	2.34	0.8	3.44	222	198	
23	296	506	298	3.2	1.74	0.92	1.17	2195	1271	
24	322	1291	799	0.9	0.89	0.68	1.89	1867	927	
25	314	689	874	4	1.59	0.6	1.46	1674	679	
26	308	4322	878	0.5	1.18	0.52	1.96	1610	624	
27	338	349	523	2	2.04	0.74	1.76	1122	608	
28	324	1574	560	0.6	1.15	0.72	1.81	1526	799	
29	309	833	449	0.9	0.70	0.93	1.82	2227	1476	
30	339	1893	1104	1	0.85	0.59	2.32	1005	487	
31	372	1790	214	0.3	1.66	0.44	2.25	666	243	

<sup>a</sup> $cC_{\max,p,u}$  values from eq 1 are scaled lower by  $\sim 0.58$  log units based upon empirical correlation. Further information is provided in the Supporting Information, Table 1, which includes values for  $cf_{u,p}$  and  $cf_{u,b}$  as described in eqs 2 and 3; values for  $cT_{1/2}$  (from  $cVD_{ss}$ ,  $cRLM$ ,  $cf_{u,p}$  and  $cf_{u,b}$ ) and  $cT_{max}$  (from  $cT_{1/2}$ ), which are necessary parameters for eq 1; full calculation of  $cC_{\max,p,u}$  and  $cC_{\max,b,u}$  as described in eqs 1–6; and a full calculation of these parameters using experimental data for comparison. In this table and subsequent figures, the letter “c” is added as a prefix to designate computed values. <sup>b</sup>Non-CNS controls. <sup>c</sup>Nonkinase inhibitor.

Table 2. Example  $C_{\max,u}$  Calculation Workflow<sup>a</sup>

Compound	Required parameters for calculated $C_{\max,p,u}$							cBA		$cC_{\max,b,u}$
	dose	cVDss	MW	cELOGD	$cf_{u,p}$	cRLM	CL <sub>blood</sub>	$c(C_b/C_p)$	$cf_{u,b}$	
13	10	1.95	359.8	3.19	0.09	169.7	14.7	0.91	0.036	
	1. $\frac{dose}{VD_{ss}} = 5128$	2. $e^{-\frac{\ln(2)}{T_{1/2}} \times T_{max}} = 0.63$	3. $\frac{f_{u,p}}{MW} = 0.25$	$C_{\max,p,u} = 5128 \times 0.63 \times 0.25 = 803 \text{ nM} = 309 \text{ nM, scaled.}$	$cBA = c(C_b/C_p) \times (f_{u,b}/f_{u,p}) = (0.91) \times (0.40) = 0.364$	$cC_{\max,p,u} \times cBA = 803 \times 0.364 = 292 \text{ nM}$				
Details for exponential term.							Units.			
$Cl_{int,u} = \frac{cRLM}{f_{mic,u}} = \frac{169.7}{0.82} = 206.7$ ; $Cl_{blood} = \frac{70 \times Cl_{int,u} \times f_{u,p}}{70 + Cl_{int,u} \times f_{u,p}} = \frac{1302}{88.6} = 14.7$							dose [mg/kg]			
$T_{1/2} = \frac{\ln(2) \times VD_{ss}}{Cl_{blood}} = 1.5$ ; $T_{max} = \frac{\ln(2.6 \times T_{1/2})}{Ka - \ln(2)/T_{1/2}} = 1.0$							cVDss [l/kg]			
							cRLM [ml/min/kg]			

<sup>a</sup>Calculated properties required for  $C_{\max,u}$  calculations are provided for compound 13 (Table 1). The workflow shows eq 1 split into three parts. Further details and explanation can be found in the Supporting Information.

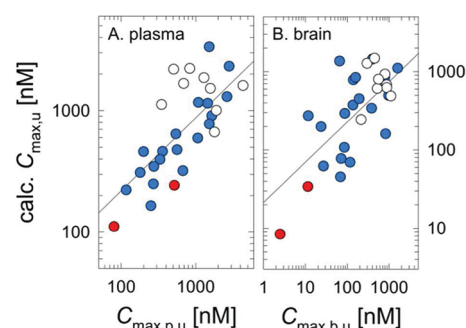


**Figure 3.** Measured vs computational predictions of  $C_{\max,u}$  values at 10 mg/kg SC dosing. (A) Refers to the measured free plasma ( $C_{\max,p,u}$ ; x-axis) vs computed free plasma ( $cC_{\max,p,u}$  via eq 1; y-axis) concentrations. (B) Refers to the measured free brain ( $C_{\max,b,u}$ ; x-axis) vs computed free brain ( $cC_{\max,b,u}$  via eq 2; y-axis) concentrations. All plots are colored using filled blue/red symbols to designate compounds tested before model construction and open/white symbols to designate compounds tested after model construction. Non-CNS kinase inhibitors are highlighted in red in the scatter plots and are considered part of the “training” set. A good correlation between experiment and predicted  $\log(C_{\max,p,u})$  values ( $R^2 = 0.55$ ;  $MSE = 0.10$ ) is observed. The correlation between experimental and predicted  $\log(C_{\max,b,u})$  values is only slightly lower ( $R^2 = 0.46$ ;  $MSE = 0.29$ ).

and  $cC_{\max,b,u}$  values on the y-axis. Both plots in Figure 3 are colored using filled symbols to designate compounds tested previous to the construction and use of the  $C_{\max,u}$  models and open symbols to designate compounds tested after model construction. A majority of prospectively designed compounds were found to have higher  $C_{\max,b,u}$  values on this normalized dose scale. In fact, only one compound was designed and synthesized with a predicted  $C_{\max,b,u}$  less than 300 nM. Furthermore, the extent of CNS exposure can be calculated to yield a BA value, which may guide design to either decrease or increase CNS exposure, depending on the desired objective. This method may allow for better perspective design, rank order of real compounds to be tested in vivo, and reduction of the number of in vivo cycles required to identify a compound with desirable exposure levels.

To better understand the factors that drive the maximum concentration values, the correlation coefficients between the observed concentrations to the component models are shown in Table 3. Free plasma levels are most correlated with  $cf_{u,p}$  and

**Table 3. Correlation Coefficients for Individual Component Models to Observed Concentrations**

	$C_{\max,p,u}$ (nM)	$C_{\max,b,u}$ (nM)
$cVD_{ss}$	0.26 <sup>b</sup>	0.02
$cC_b:C_p$	0.00	0.43 <sup>b</sup>
$cf_{u,p}$	0.41 <sup>b</sup>	0.19 <sup>a</sup>

<sup>a</sup> $p < 0.05$ . <sup>b</sup> $p < 0.005$ .

$cVD_{ss}$ , while free brain concentrations correlate with both  $cC_b:C_p$  and, to a lesser extent,  $cf_{u,p}$ . Interestingly, the correlation between  $C_{\max,b,u}$  and  $cf_{u,p}$  is positive, meaning that as the compound's free fraction increases, so does the observed free brain concentrations. This may have implications for compounds targeting non-CNS indications, since, in those instances, moderating  $cf_{u,p}$  may help to avoid CNS related side effects.

The predictive ability of these models is likely aided by the fact that a majority of the compounds in the “training” and “test” sets are low  $VD_{ss}$  compounds of similar structure (i.e., kinase inhibitors) with relatively limited transporter liability. The prediction of  $C_{\max,p,u}$  and  $C_{\max,b,u}$  values may be more difficult if accurate values for  $VD_{ss}$  and BA cannot be reliably attained from those underlying computational models. In our experience, these difficulties are more likely to be encountered in chemical classes with higher volumes and/or transporter-mediated CNS efflux issues.

It is important to note that this methodology may also be used in conjunction with existing experimental data, rather than simply as a replacement. For instance, when in vitro data exist for compounds [ $f_{u,p}$ ,  $f_{u,b}$ , rat liver microsome (RLM)], in addition to total brain exposure ( $C_b:C_p$ ), the computed volume of distribution and microsomal binding models is capable of filling in the gaps. This correlation is shown in Figure 4a.

$$\log(C_{\max,p,u}) = -0.36 + 1.01 \times \log(\text{proj-}C_{\max,p,u}) \quad (7)$$

$$\log(C_{\max,b,u}) = -0.23 + 0.96 \times \log(\text{proj-}C_{\max,b,u}) \quad (8)$$

From these relationships, there is a very reasonable agreement between the observed free drug concentrations in both plasma and brain with the values projected using eqs 3 and 4 ( $R^2$  values of 0.84 and 0.93 for  $C_{\max,p,u}$  and  $C_{\max,b,u}$  respectively).

Finally, we provide further validation of this method via the calculation of total plasma concentration ( $C_{\max,p}$ ) of a drug following a single oral dose. Here, the concentrations are computed from measured values taken from the literature and depend primarily on the observed  $VD_{ss}$  and  $F$ . Adjusting eq 1 for single oral dosing yields:

$$C_{\max,p} = \frac{\text{dose}}{VD_{ss}} \times e^{-\left[\frac{\ln(2)}{T_{1/2}} \times T_{\max}\right]} \times \frac{1}{MW} \times F \quad (9)$$

As before, the normalization of concentration and dose to a single value (10 mg) allows for the comparison of the relative exposure of many types of drugs. Figure 4b compares these normalized drug concentrations with those projected from the reported  $VD_{ss}$  and  $F$ . Compounds with low  $F$ , displayed as red symbols, were the most difficult to project using eq 9. Compounds with moderate (>30%) or high (>70%)  $F$  are well correlated ( $R^2 = 0.75$ ) using projected values from known  $VD_{ss}$  and human  $CL_{int,u}$  values. With this method, we estimate intrinsic clearance values,  $CL_{int,u}$  via a correction for microsomal binding as described by Gao et al.<sup>17</sup> For compounds with good  $F$ , it is reassuring to note that the  $C_{\max,p}$  does follow the trend defined by the ratio of dose and  $VD_{ss}$ . This correlation underscores the value of having a reasonable means for computing  $VD_{ss}$  and clearance ( $CL_{int}$ ) for prospective design of chemical compounds.

We have shown that the appropriate combination of computational ADME models are capable of reproducing experimentally measured compound concentrations. For this work, we have focused on compound concentrations following a single subcutaneous dose. We feel that the direct computation of  $C_{\max,b,u}$  from molecular structure is useful for the estimation of compound exposure and extent of CNS penetration. This model may be generally useful in designing compounds for improved  $C_{\max,b,u}$  and BA and has been successfully used to identify compounds at the drug design stage for the CNS CK1 $\delta/\epsilon$  program. Through leveraging the model developed

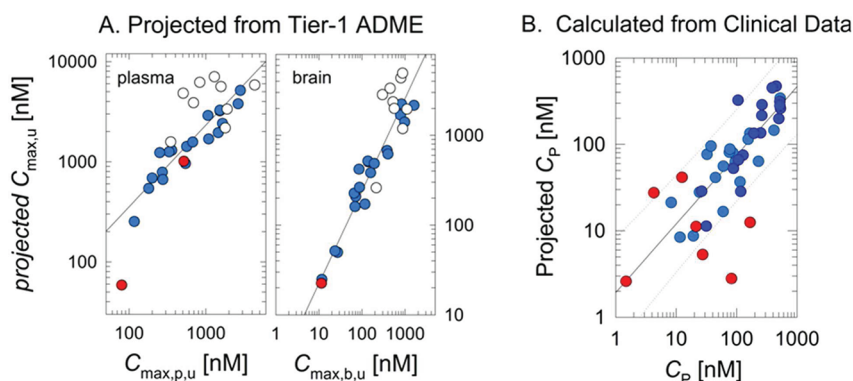


**Figure 4.** (a) Observed and projected  $C_{\max,u}$  values for a normalized SC dose (10 mg/kg). Data are provided in the Supporting Information, Table 1. (b) Observed and projected maximum concentration values normalized to 10 mg dose. Compounds with low bioavailabilities ( $F < 30\%$ ) are displayed as red symbols. Compounds with moderate ( $>30\%$ ) or high ( $>70\%$ ) bioavailability are displayed as light and dark blue symbols. Data used for this analysis are included in the Supporting Information, Table 2 (derivation of end points from literature sources), and Supporting Information, Table 3 (limited data, full referencing of experimental data; including the end points % hFu, VD<sub>ss</sub>,  $F$ ,  $C_{\max}$ ).

herein, along with the recently disclosed CNS multiple parameter optimization (MPO) desirability method,<sup>18</sup> several optimal compounds were identified and screened in an in vivo circadian rhythm model (data to be discussed elsewhere).

## ■ ASSOCIATED CONTENT

### 📄 Supporting Information

Details of the methodology, explicit  $C_{\max,u}$  calculations, and input parameters. This material is available free of charge via the Internet at <http://pubs.acs.org>.

## ■ AUTHOR INFORMATION

### Corresponding Author

\*E-mail: [scot.mente@pfizer.com](mailto:scot.mente@pfizer.com).

### Notes

The authors declare no competing financial interest.

## ■ ACKNOWLEDGMENTS

We gratefully acknowledge Xinjun Hou, Ivan Efremov, and Anabella Villalobos for careful editing of this manuscript.

## ■ ABBREVIATIONS

ADME, absorption, distribution, metabolism, excretion; B/P and  $C_b:C_p$ , total brain-to-plasma ratio; BA, brain availability;  $C_{\max,b,w}$  maximum unbound brain compound concentration;  $C_p$ , total plasma compound concentration;  $C_{\max,p,w}$  maximum unbound plasma compound concentration;  $C_{\max,w}$  maximum unbound compound concentration; CNS, central nervous system;  $f_{u,b}$ , fraction unbound in brain;  $f_{u,p}$ , fraction unbound in plasma;  $F$ , percent bioavailable; MPO, multiple parameter optimization; RLM, rat liver microsome; SC, subcutaneous; VD<sub>ss</sub>, steady-state volume of distribution

## ■ REFERENCES

- (1) Lipinski, C. A.; Lombardo, F. Experimental and Computational Approaches to Estimate Solubility and Permeability in Drug Discovery and Development Settings. *Adv. Drug Delivery Rev.* **1997**, *23*, 3–26.
- (2) Gleeson, M. P. Generation of a Set of Simple, Interpretable ADMET Rules of Thumb. *J. Med. Chem.* **2008**, *51*, 817–834.
- (3) Leeson, P. D.; Springthorpe, B. The influence of drug-like concepts on decision-making in medicinal chemistry. *Nat. Rev. Drug Discovery* **2007**, *6*, 881–890.

- (4) Lewis, M. L.; Cucurull-Sanchez, L. Structural pairwise comparisons of HLM stability of phenyl derivatives: Introduction of the Pfizer metabolism index (PMI) and metabolism-lipophilicity efficiency (MLE). *J. Comput.-Aided Mol. Des.* **2009**, *23*, 97–103.

- (5) Yoshida, F.; Topliss, J. G. QSAR model for drug human oral bioavailability. *J. Med. Chem.* **2000**, *43*, 2575–2585.

- (6) Mente, L. A recursive-partitioning model for blood–brain barrier permeation. *J. Comput.-Aided Mol. Des.* **2005**, *19*, 465–481.

- (7) Adenot, M.; Lahana, R. Blood-Brain Barrier Permeation Models: Discriminating between Potential CNS and Non-CNS Drugs Including P-Glycoprotein Substrates. *J. Chem. Inf. Comput. Sci.* **2004**, *44*, 239–248.

- (8) Luco, J. M. Prediction of the Brain-Blood Distribution of a Large Set of Drugs from Structurally Derived Descriptors Using Partial Least-Squares (PLS) Modeling. *J. Chem. Inf. Comput. Sci.* **1999**, *39*, 396–404.

- (9) Lombardo, F.; Blake, J. F. Computation of Brain-Blood Partitioning of Organic Solutes via Free Energy Calculations. *J. Med. Chem.* **1996**, *39*, 4750–4755.

- (10) Abraham, M. H.; Chadha, H. Hydrogen Bonding: 33. Factors That Influence the Distribution of Solutes between Blood and Brain. *J. Pharm. Sci.* **1994**, *83*, 1257–1268.

- (11) Berellini, G.; Springer, C. In Silico Prediction of Volume of Distribution in Human Using Linear and Nonlinear Models on a 669 Compound Data Set. *J. Med. Chem.* **2009**, *52*, 4488–4495.

- (12) Lombardo, F.; Shalaeva, M. Y. ElogD<sub>out</sub>: A Tool for Lipophilicity Determination in Drug Discovery. 2. Basic and Neutral Compounds. *J. Med. Chem.* **2001**, *44*, 2490–2497.

- (13) Lanevskij, K.; Dapkunas, J. QSAR analysis of blood–brain distribution: The influence of plasma and brain tissue binding. *J. Pharm. Sci.* **2011**, *100*, 2147–2160.

- (14) Fridén, M.; Bergström, F. Measurement of Unbound Drug Exposure in Brain: Modeling of pH Partitioning Explains Diverging Results between the Brain Slice and Brain Homogenate Methods. *Drug Metab. Dispos.* **2011**, *39*, 353–362.

- (15) Chen, H.; Winiwarter, S. In silico prediction of unbound brain-to-plasma concentration ratio using machine learning algorithms. *J. Mol. Graphics Modell.* **2011**, *29*, 985–995.

- (16) Kalvass, J. C.; Maurer, T. S. Use of Plasma and Brain Unbound Fractions to Assess the Extent of Brain Distribution of 34 Drugs: Comparison of Unbound Concentration Ratios to in Vivo P-Glycoprotein Efflux Ratios. *Drug Metab. Dispos.* **2007**, *35*, 660–666.

- (17) Gao, H.; Yao, L. In Silico Modeling of Nonspecific Binding to Human Liver Microsomes. *Drug Metab. Dispos.* **2008**, *36*, 2130–2135.

- (18) Wager, T. T.; Chandrasekaran, R. Y. Defining Desirable Central Nervous System Drug Space through the Alignment of Molecular Properties, in Vitro ADME, and Safety Attributes. *ACS Chem. Neurosci.* **2010**, *1*, 420–434.